Am J Cancer Res 2022;12(6):2850-2862
www.ajcr.us /ISSN:2156-6976/ajcr0143887

Original Article

Ipatasertib, an oral AKT inhibitor, inhibits cell proliferation and migration, and induces apoptosis in serous endometrial cancer

Lindsey Buckingham[1], Tianran Hao[1], Jillian O'Donnell[1], Ziyi Zhao[1,2], Xin Zhang[1,2], Yali Fan[1,2], Wenchuan Sun[1], Yingao Zhang[1], Hongyan Suo[1,2], Angeles Alvarez Secord[3], Chunxiao Zhou[1,4], Victoria Bae-Jump[1,4]

[1]Division of Gynecologic Oncology, University of North Carolina at Chapel Hill, Chapel Hill, NC, USA; [2]Department of Gynecologic Oncology, Beijing Obstetrics and Gynecology Hospital, Capital Medical University, Beijing Maternal and Child Health Care Hospital, Beijing, China; [3]Division of Gynecologic Oncology, Department of Obstetrics and Gynecologic, Duke Cancer Institute, Duke University, Durham, NC, USA; [4]Lineberger Comprehensive Cancer Center, University of North Carolina at Chapel Hill, Chapel Hill, NC, USA

Received May 3, 2022; Accepted May 27, 2022; Epub June 15, 2022; Published June 30, 2022

Abstract: Ipatasertib (IPAT) is an orally administered, selective protein kinase B (AKT) inhibitor with promising data in solid tumors in both pre-clinical studies and clinical trials. Given that the PI3K/AKT/mTOR pathway is frequently dysregulated in uterine serous carcinoma (USC), we aimed to explore the functional impact of IPAT on anti-tumorigenic activity in USC cell lines and primary cultures of USC. We found that IPAT significantly inhibited cell proliferation and colony formation in a dose-dependent manner in USC cells. Induction of cell cycle arrest and apoptosis was observed in IPAT-treated ARK1 and SPEC-2 cells. Treatment with IPAT resulted in reduced adhesion and invasion of both cell lines with a concomitant decrease in the expression of Snail, Slug, and N-Cadherin. Compared with single-drug treatment, the combination of IPAT and paclitaxel synergistically reduced cell proliferation and increased the activity of cleaved caspase 3 in both cell lines. Additionally, IPAT inhibited growth in four of five primary USC cultures, and three of five primary cultures also exhibited synergistic growth inhibition when paclitaxel and IPAT were combined. These results support that IPAT appears to be a promising targeted agent in the treatment of USC.

Keywords: Ipatasertib, uterine serous carcinoma, cell proliferation, synergy, paclitaxel

Introduction

In the United States, it is projected that more than 65,950 women will be diagnosed with endometrial cancer in 2022, and nearly 12,550 will die of their disease [1]. Most women are diagnosed with endometrioid cancers at early stages and can be cured with surgery alone. Uterine serous carcinoma (USC) comprises approximately 10% of endometrial cancer cases; however, it is more often diagnosed at advanced stages, and recurrence after initial treatment accounts for 80% of endometrial cancer deaths [2]. Due to the high recurrence rate and poor prognosis inherent to USC, there is an urgent need to develop new treatment regimens for this deadly disease.

USC has a distinct molecular biological profile compared with endometrioid endometrial cancer. Mutations in *PIK3CA*, *FBXW7*, and *PTEN* have been found in 29%, 12%, and 7% of USC tumors respectively, indicating that the *PI3K/AKT/mTOR* pathway is frequently dysregulated in USC [3, 4]. Recent studies found that *PIK3CA* mutations induced high PIK3CA oncogenic activity via the AKT signaling pathway, resulting in malignant transformation and aggressive behavior in endometrial cancer [3, 5, 6]. Additionally, cancer cells including USC cells with identified *PIK3CA* mutations or high PI3K/AKT activity were more sensitive to PI3K/AKT/mTOR inhibitors [7, 8]. Taken together, these results suggest potential benefit of targeted therapy with specific small molecule inhibitors acting on the PI3K/AKT/mTOR pathway in USC. In recent years, several PI3K/AKT/mTOR inhibitors have shown promising results in USC cells and mouse models, and multiple clinical trials are ongoing [8-11].

Ipatasertib (IPAT) is an orally administered ATP-competitive pan-AKT inhibitor of all three isoforms of phosphorylated AKT [12] (p-AKT). Unlike its mTOR-inhibitor predecessors, IPAT displays selectivity for its molecular target and potent inhibition of AKT signaling and associated downstream targets [13, 14]. Targeting the PI3K/AKT/mTOR pathway by IPAT results in decreased cancer cell proliferation and tumor growth in variety of tumor models in *vitro and in vivo* [15, 16]. In pre-clinical studies, IPAT has also shown synergy with cytotoxic agents, particularly paclitaxel, in multiple cancer cell lines [15, 17, 18]. Clinical phase I trials showed that IPAT alone or IPAT in combination with chemotherapy or hormonal therapy was safe and well tolerated in patients with solid tumors [19, 20]. The recent phase II LOTUS trial demonstrated that the combination of IPAT with paclitaxel improved progression free survival in patients with *PIK3CA/AKT1/PTEN* altered triple-negative breast cancer [21]. Currently, multiple phase II/III trials are underway investigating IPAT's activity alone and in combination in solid tumors including endometrial cancer. The purpose of this study is to elucidate the anti-proliferative efficacy of IPAT alone and in combination with paclitaxel on USC cell lines and in primary cultures.

Methods

Cell culture and reagents

Two cell lines representing USC were utilized for all experiments: SPEC-2 (*PTEN* null) and ARK1 (*PTEN* wild type, *PI3K/AKT* alterations) [22]. SPEC2 cells were maintained in DMEM/F12 medium with 10% fetal bovine serum (FBS). ARK1 cells were maintained in RPMI 1640 medium with 10% FBS. All media contained penicillin (100 U/mL) and streptomycin (100 µg/mL). Cells were cultured in a humidified, 5% CO_2 incubator at 37°C. IPAT was obtained from Genentech, Inc. Antibodies were purchased from Cell Signaling Technology (Beverly, MA). Enhanced chemiluminescence Western blotting detection reagents were purchased from Amersham (Arlington Heights, IL). All other reagents and chemicals were purchased from Sigma (St. Louis, MO).

MTT assay

The SPEC-2 and ARK1 cells were plated in 96-well plates at a concentration of 3-8×10^3 cells/well and grown for 24 hours. Cells were then treated with varying concentrations of IPAT for 72 hours. A volume of 5 µL/well of MTT (5 mg/mL) was added at the end of treatment, and plates incubated for 1 hour. The MTT reaction was then terminated by addition of 100 µL/well of DMSO. Absorption was measured at a wavelength of 575 nm with a Tecan microplate reader (Morrisville, NC). The effect of IPAT on cell proliferation was calculated as a percentage of control. Control wells on the same 96-well plates were treated with DMSO only. IC_{50} values were calculated using the AAT Bioquest calculator. Experiments were performed in triplicate to assure consistency of results. For synergy studies, the cells were treated with IPAT, paclitaxel (TAX), or the combination for 72 hours in 96-well plates. Effects of IPAT and TAX were calculated as a percentage of control. Control wells on the same 96-well plates were treated with DMSO only. The Combination Index (CI) was calculated using the Bliss Independence model to determine whether the drug effects were additive (CI=1), synergistic (CI<1), or antagonistic (CI>1) [23]. Each experiment was repeated in triplicate for consistency of results.

Colony assay

The SPEC-2 and ARK1 cells were plated in 6-well plates at a concentration of 150 cells/well and 100 cells/well, respectively. After 24 hours, cells were treated with varying concentrations of IPAT for 36 hours. The plates were grown for 14 days, with media exchange every third day. Cells were treated with a mixture of 6.0% glutaraldehyde and 0.5% crystal violet to stain individual colonies. The colonies were counted by bright-field microscopy. Each experiment was performed in triplicate for consistency of results.

Cell cycle assay

The SPEC-2 and ARK1 cells were plated in 6-well plates at a concentration of 2-4×10^5 cells/well and grown for 24 hours. Cells were treated with varying concentrations of IPAT for 30 hours and then harvested from plates. Pellets were washed in PBS twice, and cells were fixed with 90% methanol and kept in -20°C until cell cycle analysis. Before analysis, cells were centrifuged and the pellet resuspended using a solution containing propidium iodide (PI), RNase, and Triton X-100 for 30 min-

utes. Cell cycle progression was analyzed by imaging cytometry using Cellometer Vision (Nexcelom Bioscience LLC). This experiment was performed in triplicate to assess for consistency of results.

Cleaved caspase-3, 8, and 9 ELISA assays

The SPEC-2 and ARK1 cells were plated in 6-well plates at a concentration of 3×10^5 cells/well for 24 hours. Cells were then exposed to varying concentrations of IPAT for 18 hours. 150-180 µL of 1X caspase lysis buffer was added to each well. Protein concentration was analyzed using the BSA assay. Lysates (10-15 µg) were transferred to black, clear bottom, 96-well plates and incubated with reaction buffer and 200 µM of caspase substrates Ac-DEVD-AMC (AAT Bioquest, Sunnyvale, CA) for 30 min. Fluorescence of each well was analyzed using the Tecan microplate reader (Ex/Em=400/505 nm). This experiment was performed in triplicate to ensure consistency of results.

Adhesion assay

Each well of a 96-well plate was coated with 100 µL of laminin-1 (10 µg/mL) and allowed to incubate at 37°C for one hour. The fluid was then aspirated, and 200 µL/well of blocking buffer was added. Plates were incubated for 45 minutes at 37°C, after which wells were washed with PBS and placed on ice. The SPEC-2 and ARK1 cells were harvested, washed, and centrifuged. The cells were then resuspended in PBS and added to the wells at a density of 25000 cells/well along with varying concentrations of IPAT. Plates were incubated for 1 hour at 37°C. Media was aspirated from the wells, and cells were fixed with 100 µL of 5% glutaraldehyde/well and incubated for 30 minutes at room temperature. Adherent cells were washed with PBS and stained with 0.1% crystal violet solution (100 µL/well) for 30 minutes. Wells were then washed with sterile water and 100 µL/well of 10% acetic acid was added to solubilize the dye. Plates were shaken for 5 minutes and absorbance was measured at 575 nm using a Tecan microplate reader. Experiments were performed in triplicate to ensure consistency.

Wound healing assay

The SPEC-2 and ARK1 cells were plated in 6-well plates at a concentration of 4×10^5 cells/well and grown for 24 hours or until >80% confluency as assessed by microscopy. Uniform, cruciate wounds through the cell monolayer were created using a 20 µL pipette tip. Cells were washed and treated with varying concentrations of IPAT for 24 to 72 hours. Photographs were taken at 24, 48, and 72 hours during treatment. The width of wounds was measured and analyzed using the software ImageJ (National Institutes of Health; Bethesda, MD). Experiments were performed in triplicate to ensure consistency of results.

Western immunoblotting

The SPEC-2 and ARK1 cells were plated at a concentration of 2.5×10^5 cells/well and grown for 24 hours or until 60-70% confluency reached. Cells were then treated with varying concentrations of IPAT for 18-32 hours. Cell lysates were prepared in RIPA buffer, and isolated protein solutions were kept on ice. BSA assay was used to determine the concentration of protein. Equal amounts of protein were separated by gel electrophoresis and transferred onto a polyvinylidene difluoride (PVDF) membrane. Membranes were blocked with 5% non-fat milk solution and incubated with a 1:1000 to 2000 dilution of primary antibodies overnight at 4°C. Membranes were then washed and incubated with secondary, peroxidase-conjugated antibodies for 1 hour. Antibody binding was detected using an enhanced chemiluminescence detection system on the ChemiDoc Image System (Bio-Rad, Hercules, California). After developing, the membranes were stripped and re-probed using anti α-tubulin or β-actin antibodies to confirm equal protein loading. Intensity for each band was measured and normalized to α-tubulin as an internal control. Experiments were performed in triplicate to ensure consistency of results.

Primary culture of human-derived USC

After obtaining informed consent, tumor tissues were collected from patients with USC at the time of hysterectomy. Tumors were identified by trained pathologists, and 5×5 mm cubed specimens were placed in culture media with antibiotics for transfer. Tissues were then digested in 0.2% collagenase I for 30-60 min in a 37°C water bath with shaking. After two centrifugations with PBS solution, cells were seeded into 96-well plates, and cell proliferation was measured by MTT assay 72 hours after treatment with IPAT.

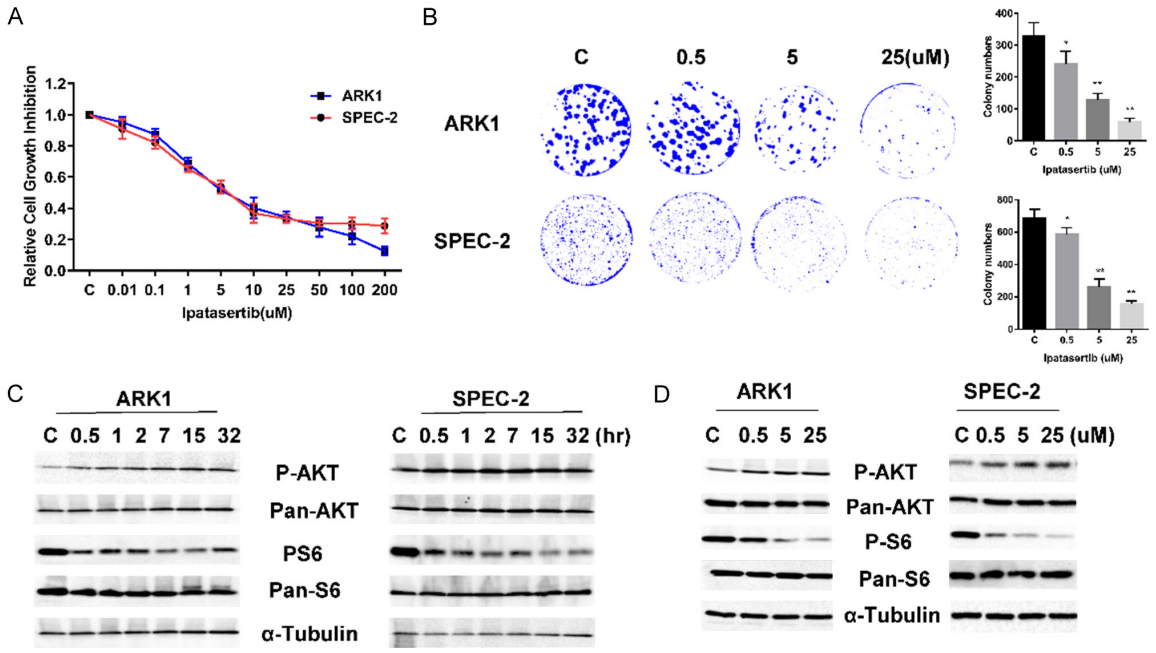

Figure 1. IPAT inhibits cell proliferation in USC cell lines. The ARK1 and SPEC-2 cells were treated with increasing concentrations of IPAT for 72 hours and subjected to the MTT assay in 96 well plates. IPAT significantly inhibited cell proliferation in a dose-dependent manner in both cell lines (A). Colony formation assays showed that IPAT reduced colony formation in both cell lines (B). Similar results were obtained from three independent experiments. Western immunoblotting was used to evaluate the effect of IPAT on expression of p-AKT and p-S6 in the ARK1 and SPEC-2 cells. IPAT increased the expression of p-AKT and decreased the expression of p-S6 in a time-dependent fashion in both cell lines (C). IPAT treatment for 24 hours increased p-AKT expression and downregulated p-S6 expression in a dose-dependent manner in both cell lines (D).

Statistical analysis

Data are reported as mean ± SD. Statistical significance was analyzed by a two-sided unpaired Student's t-test from at least three experimental replicates. *P*-values of <0.05 were considered to have significant differences. GraphPad Prism 6 (La Jolla, CA USA) was used for all graphs and significance tests.

Results

IPAT inhibits cellular proliferation in USC cells

To observe whether IPAT exhibits inhibitory activity against USC cells, we used different concentrations of IPAT to treat *PTEN* wild type ARK1 and *PTEN* null SPEC-2 cells for 72 hours. Cellular viability was measured using the MTT assay. IPAT significantly reduced cell viability in a dose-dependent manner in both cell lines. Mean IC_{50} values were 6.62 μM for ARK1 and 2.05 μM for SPEC-2, respectively (**Figure 1A**). Given that colony formation assay is the gold standard to evaluate the ability of single cells to survive and the effects of cytotoxic agents on cancer cell viability [24], the clonogenicity of ARK1 and SPEC-2 cells was assessed. Cells were exposed to IPAT for 24 hours and then cultured for another two weeks. IPAT exhibited inhibitory effects on the clonogenicity of the two USC cell lines in a dose-dependent fashion. Compared to controls, a 25 μM concentration of IPAT reduced colony formation by 82.32% in ARK1 cells and 77.05% in SPEC-2 cells, P<0.01, (**Figure 1B**). These results suggest that USC cells are sensitive to IPAT.

The effect of IPAT on phosphorylation of AKT and S6 was determined by Western blotting. ARK1 and SPEC-2 cells were treated with 10 μM of IPAT for a time course of up to 32 hours. Consistent with other studies, IPAT induced an increase in expression of p-AKT (Ser473) in a time-dependent fashion in both cell lines. Increased expression in this setting indicates engagement and binding of IPAT with the p-AKT complex. Downstream, however, phosphorylated-S6 (p-S6) expression was downregulated in a time-dependent fashion indicating overall

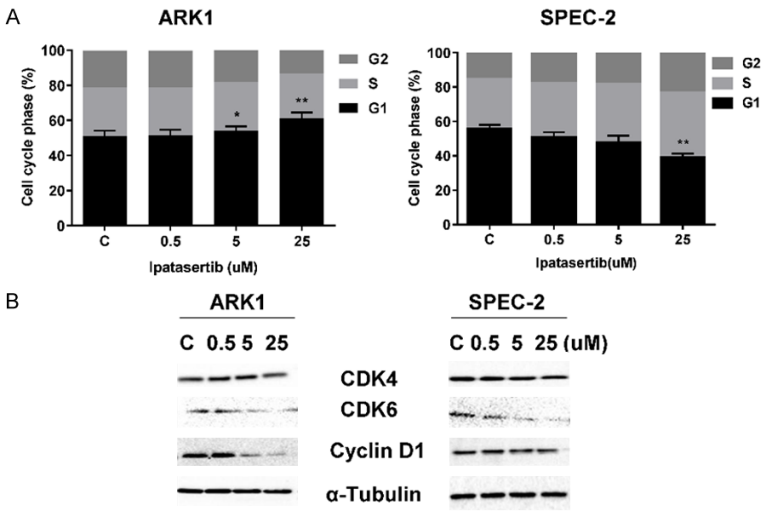

Figure 2. IPAT induces cell cycle arrest in USC cell lines. The ARK1 and SPEC-2 cells were incubated with vehicle or IPAT at 0.5, 5, or 25 μM for 30 hours. Cell cycle distribution was analyzed by Cellometer. IPAT induced cell cycle G1 arrest in the ARK1 cells and G2 arrest in the SPEC-2 cells (A). Western blotting analysis of the cell cycle regulatory proteins CDK4, CDK6, and Cyclin D1 was performed on lysates from the ARK1 and SPEC-2 cells after 24 hours of IPAT treatment (B). α-Tubulin was included as a loading control. Error bars represent SEM from triplicates.

inhibition of the AKT/mTOR/S6 pathway (**Figure 1C**). Consistent with the results above, treatment with IPAT at different concentrations for 24 hours increased the expression of p-AKT and decreased p-S6 expression in a dose-dependent manner in both cell lines (**Figure 1D**).

IPAT induces cell cycle arrest

Given that IPAT targets cell proliferation through the AKT/mTOR pathway, cell cycle arrest was measured in both cell lines. ARK1 and SPEC-2 cell lines were treated with varying concentrations of IPAT for 30 hours. IPAT induced cell cycle arrest in the G1 phase in ARK1 cells and G2 phase in SPEC-2 cells in a dose-dependent fashion. After treatment with 25 μM IPAT, the proportion of ARK1 cells in G1 increased from ~50% to ~58%, whereas in SPEC-2 cells, the proportion of cells in G2 phase increased from ~15% to ~23%, and G1 phase arrest decreased from ~55% to ~38% (**Figure 2A**, $P<0.05$). To further clarify the effect of IPAT on cyclins, we performed Western immunoblotting for CDK-6, CDK-4, and Cyclin D1. The expression of CDK-6, CDK-4, and Cyclin D1 all decreased in a dose-dependent manner in both cell lines after treatment with IPAT for 24 hours (**Figure 2B**).

IPAT induces apoptosis in USC cells

To determine the effect of IPAT on the induction of apoptosis, we performed ELISA assays and Western blotting analysis to detect apoptosis in the USC cells. Treatment of ARK1 and SPEC-2 cells with IPAT at different doses for 18 hours induced increased activity of cleaved caspase 3, cleaved caspase 8, and cleaved caspase 9 in a dose-dependent manner. In ARK1 cells, 25 μM IPAT induced cleaved caspase 3, 8 and 9 activities by 1.75 ($P<0.05$), 1.51 ($P<0.01$), and 1.69 ($P<0.05$) fold respectively, when compared to control cells. In SPEC-2 cells, 25 μM IPAT increased cleaved caspase activity by 2.9, 1.59, and 1.61 fold ($P<0.01$) respectively (**Figure 3A-C**). Furthermore, Western blotting results showed that the expression of BCL-2 and MCL-1 decreased with increasing doses of IPAT in both cell lines (**Figure 3D**). These results indicate that apoptosis induced by IPAT occurs through activation of both extrinsic and intrinsic pathways in USC cells.

IPAT inhibits cell migration and invasion in USC cells

To investigate whether IPAT has anti-invasive activity in USC cells, laminin adhesion, wound healing, and transwell assays were performed in both cell lines. In the assessment of cell adhesion, ARK1 and SPEC-2 cells were incubated in laminin-coated 96-well plates and treated with different doses of IPAT for 4 hours. With 25 μM IPAT treatment, cell adhesion was decreased by 15% and 17% ($P<0.01$) in SPEC-2 and ARK1 cells, respectively (**Figure 4A**). IPAT's capacity to inhibit cell invasion was assessed using a transwell invasion assay with a matrigel-coated filter. Invasion of ARK1 and SPEC-2 cells was reduced by IPAT treatment in a dose-dependent manner (**Figure 4B**). At a dose of 25 μM, IPAT reduced cell invasion by 15.4% and 20.3% in ARK1 and SPEC-2 cells, respectively ($P<0.01$). The anti-migratory activ-

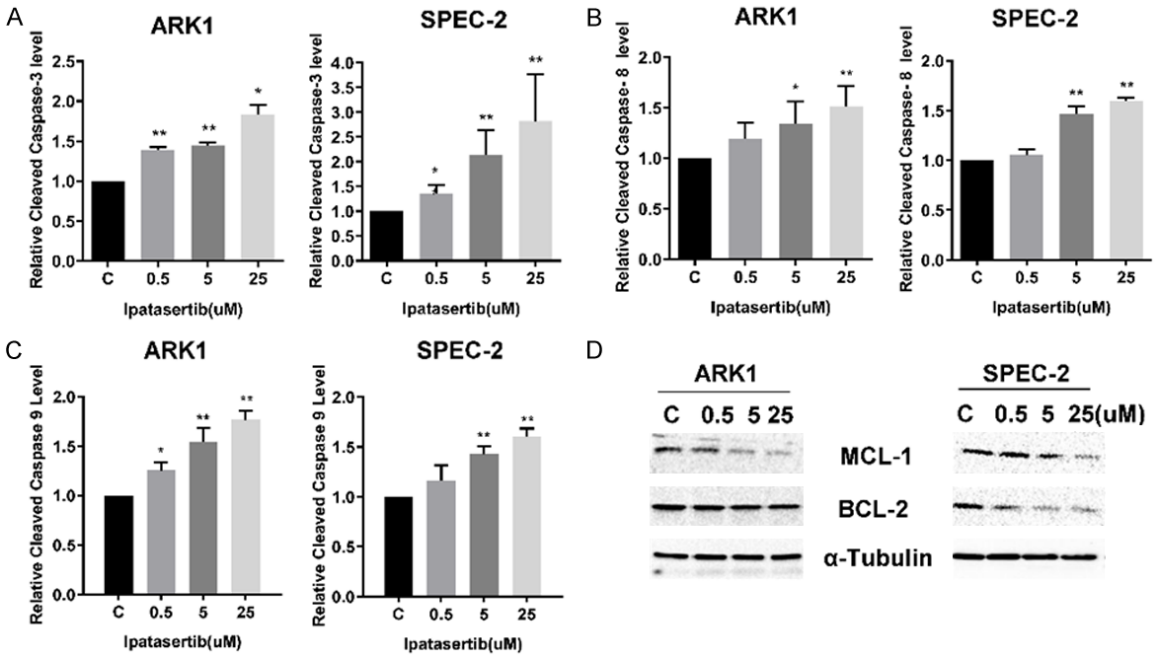

Figure 3. IPAT induces apoptosis in USC cell lines. Cleaved caspase 3, 8, and 9 were detected by ELISA assays after ARK1 and SPEC-2 cells were treated with different concentrations of IPAT for 18 hours. IPAT increased cleaved caspase 3, 8, and 9 activity in both cell lines in a dose-dependent manner (A-C). The ARK1 and SPEC-2 cells were treated with different concentrations of IPAT for 24 hours, after which the expression of MCL-1 and BCL-1 was detected by Western blotting analysis (D). *P<0.05, **P<0.01.

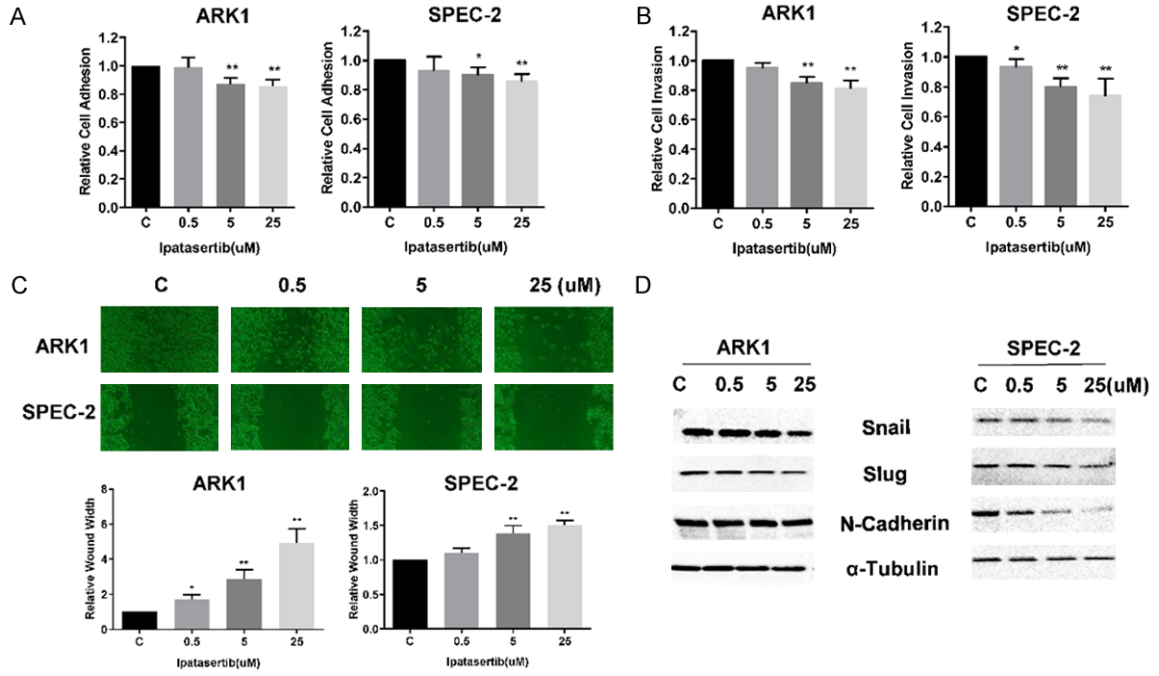

Figure 4. IPAT inhibits cell adhesion and migration in USC cell lines. After the ARK1 and SPEC-2 cells were treated with vehicle control or IPAT for 4 hours, cell adhesion was assessed by laminin assay (A). Transwell assay was used to determine the effect of IPAT on cell invasion in both cell lines after 12 hours of treatment with IPAT (B). IPAT inhibited cell adhesion and invasion in both USC cell lines. Cell migration was assessed by wound healing assay in both cell lines. The migration of ARK1 and SPEC-2 cells in a wound healing assay was impaired at both the 24 and 72 hour time-points after treatment with IPAT. Images showed the changes of migration after 48 hours of treatment (C). Western blotting showed that IPAT decreased the expression of Snail, Slug, and N-Cadherin in both cell lines (D). Each experiment was conducted in triplicate.

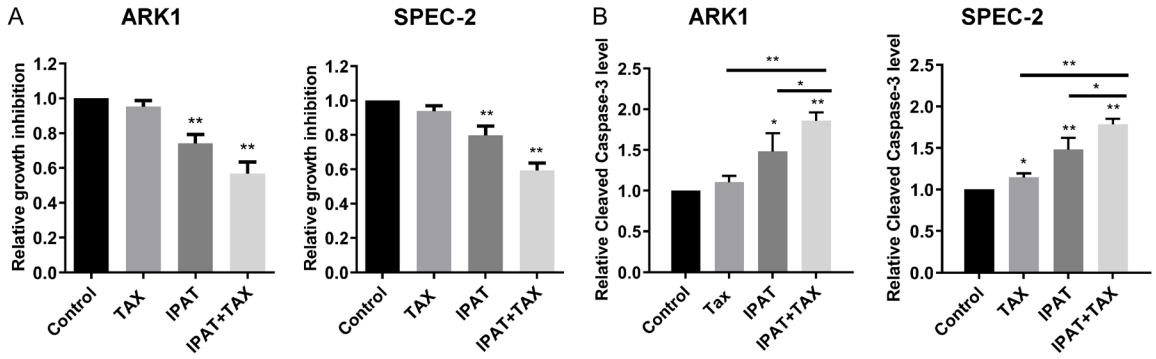

C

CI value for the combination in ARK1 cells

	IPAT 0.5	IPAT 5	IPAT 25*
Taxol 0.1	0.844171	0.876586	0.872376
Taxol 1	0.84136	1.089164	1.184501
Taxol 10*	1.337945	1.535758	1.656107

D

CI value for the combination in SPEC-2 cells

	IPAT 0.5	IPAT 5	IPAT 25*
Taxol 0.1	0.843985	0.913633	0.995241
Taxol 1	0.924342	1.037905	1.083333
Taxol 10*	1.375499	1.498164	1.48953

*** IPAT: uM, Taxol: nM**

Figure 5. IPAT displays synergy with paclitaxel in USC cell lines. The ARK1 and SPEC-2 cells were treated with 0.1 nM TAX, 0.5 μM IPAT or the combination of the two compounds for 72 hours. Cell viability was detected by MTT assay. The combination of IPAT and TAX was significantly more effective in inhibiting cell proliferation than either of the single agents alone in both cell lines (A). Combination of IPAT and TAX induced more cleavage caspase 3 activity than either IPAT or TAX alone after 18 hours of treatment (B). Both cell lines were incubated with TAX or IPAT at different concentrations as indicated for 72 hours. The CI values were analyzed by the Bliss Independence model for each combination point in ARK1 (C) and SPEC-2 cells (D).

ity of IPAT was evaluated by performing a wound healing assay on ARK1 and SPEC-2 cells. After the initial wound was created by scratching the monolayer of cells, the cells were treated with various concentrations of IPAT for 24 and 48 hours. Wound healing was slower in IPAT treated cells than in control cells in a dose-dependent manner. Treatment of cells with 25 μM IPAT for 48 hours reduced the migration of ARK1 and SPEC-2 cells up to 80.1% and 49.3%, respectively (P<0.01) (**Figure 4C**). Western blotting showed that IPAT changed the expression of epithelial-mesenchymal-transition (EMT) markers. After 24 hours of treatment, IPAT decreased the expression of Snail, Slug and N-Cadherin in both cell lines (**Figure 4B**). These results confirm that IPAT effectively suppresses both migration and invasion in USC cells *in vitro.*

IPAT displays synergy with paclitaxel

While multiple studies have shown synergy between IPAT and paclitaxel (TAX) in preclinical models including breast, prostate, and colorectal cancers [14, 15, 25], the combined effects of IPAT and TAX have not yet been studied in USC cells. To evaluate for synergy in ARK1 and SPEC-2, both cell lines were treated with three different doses (approximating IC_{20}, IC_{50} and IC_{70}) of IPAT alone, TAX alone, and the combination of the two. Cell proliferation was determined by MTT assay after 72 hours of treatment. Combination Index values (CI) were calculated by Bliss Independence model for each combination point. Dose-dependent inhibition of cell growth with IPAT or TAX alone was observed in both cell lines. The IPAT/ TAX combination doses above IC_{50} more potently reduced cell viability when compared to each agent alone (**Figure 5A**). In the ARK1 and SPEC-2 cells, 0.1 nM TAX reduced cell proliferation by 7.5% and 5.2%, respectively (P=NS), while 0.5 μM IPAT decreased proliferation by 24.4% and 20.2%, respectively (P<0.01). In both cell lines, the combination of 0.1 nM TAX and 0.5 μM IPAT was significantly more effective in inhibiting cell proliferation than each of the single agents and produced 44.3% and 40.2% inhibition (P<0.01) in ARK1 and SPEC-2 cells, respectively. Cleaved caspase 3 assay showed that the combination of IPAT and TAX more

Table 1. Patient characteristics

Cases	Age	Race	Stage	Tumor size*	Histology	HER2 (FISH)
USC1	57	Black	II	2.2	Serous	Negative
USC2	64	White	IA	3.1	Serous	N/A
USC3	62	Black	IA	0.8	Serous	Negative
USC4	84	White	IA	2.2	Serous Mixed	Negative
USC5	62	Black	IIIC1	N/A	Serous carcinosarcoma	Positive

N/A: Not reported. *Tumor diameter, Centimeter.

potently induced cleaved caspase 3 activity than either IPAT or TAX alone after 18 hours of treatment (P<0.05 and P<0.01, respectively) (**Figure 5B**). The analysis of CI values at multiple paired concentrations revealed synergistic activity in the low dose combination treatments in both cell lines (**Figure 5C**, **5D**), demonstrating that combination IPAT and TAX may have a better anti-proliferative activity against USC cells than when used as single agents.

Primarily cultured USC cells display variable responses to IPAT, paclitaxel, and combination dosing

Primary cell culture from patient-derived tumors may better predict the anti-tumorigenic activity of cytotoxic agents than immortalized cell lines. We isolated primary cancer cells derived from patients with USC for the current study. Patient characteristics are described in **Table 1**. Five total primary cell cultures of USC were treated with varying concentrations of IPAT, TAX, and combination dosing. MTT assay showed that primarily cultured USC cells experienced variable responses to IPAT and TAX after 72 hours of treatment. Four of the five primary cultures displayed decreased cell viability after treatment with IPAT. TAX inhibited cell growth to varying degrees in all cell lines, however magnitude of response varied by the individual tumors (**Figure 6A**, **6B**). Similar to findings in ARK1 and SPEC-2 cell lines, the combination of IPAT and TAX at low doses produced synergetic responses in three of five primary cultures (**Figure 6C-E**). In order to determine whether the expression of p-AKT and p-S6 was related to sensitivity to IPAT, we detected the expression of p-AKT and p-S6 using Western blotting in three untreated primary cell cultures (USC1, 2 and 3) as well as the USC cell lines (ARK1 and SPEC-2). We were unable to collect sufficient protein for Western blotting in primary cultures USC4 and 5. Western blotting revealed differential baseline expression of p-AKT and p-S6 in each case. SPEC-2 showed the highest baseline expression of p-AKT and low-moderate expression of p-S6. ARK1 cells displayed very low levels of baseline expression of p-AKT and p-S6. Primary culture USC3 showed moderate baseline expression of p-AKT and p-S6 compared to USC1 and 2 (**Figure 6F**); however, USC3 appeared to be the most sensitive to inhibition of cell proliferation (**Figure 6A**). While USC1 displayed higher baseline expression of p-AKT and p-S6, USC2 showed low expression of p-AKT and the highest expression of p-S6 (**Figure 6F**). USC1 and 2 displayed the least sensitivity to IPAT inhibition of cell proliferation. Thus, in both primary culture and immortalized cell lines, baseline expression of p-AKT and p-S6 was not only variable, but independent of cell sensitivity to inhibition by IPAT (**Figure 6F**).

Discussion

Uterine serous carcinoma is an aggressive entity with a propensity for recurrence and poor outcomes. Especially in the recurrent setting, there are few effective antitumor agents available, and until the approval of pembrolizumab in 2018, no new therapies had been approved for nearly 50 years for use in recurrent endometrial cancers. Agents targeting the PI3K/AKT/mTOR pathway are under investigation in several endometrial cancer clinical trials, due to the ubiquitous nature of alterations in this pathway in endometrial cancers including USC [17, 26]. Although promising in preclinical studies, mTOR inhibitors have fallen short of expectations in phase Ib/II trials evaluating their efficacy in recurrent endometrial cancers [13]. This is thought due to the lack of target selectivity as well as activation of alternative pathways or feedback loops that compensate for inhibition of the AKT/mTOR pathway [26]. IPAT is a highly selective inhibitor of phosphorylated AKT which competitively binds and inactivates

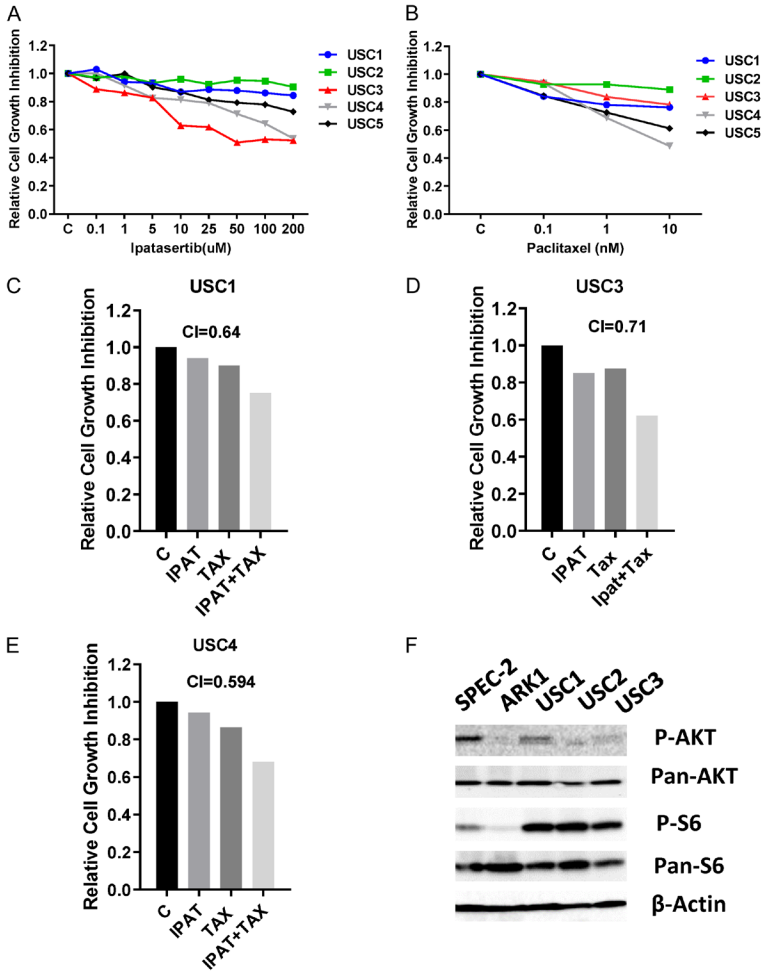

Figure 6. IPAT inhibited cell proliferation and increased the sensitivity to paclitaxel in primary cultures of USC. Five primary cultures of human USC were cultured in 96-well plates and treated with IPAT or TAX at indicated doses for 72 hours. MTT assay was used to detect cell viability (A and B). Three of five primary cultures showed synergic inhibition after combination treatment with IPAT and TAX (C-E). The SPEC-2 and ARK1 cell lines, and three primary culture cells were seeded in six well plates and cultured for 48 hours. The expression of phosphorylated AKT and S6 protein was detected by Western blotting (F). Sensitivity to IPAT was independent of the baseline expression levels of phosphorylated AKT and S6 in the established USC cell lines and the primary culture cells of USC.

the p-AKT complex and disrupts the mTOR pathway. In pre-clinical studies of several solid tumors, IPAT has shown potent anti-proliferative effects both alone and synergistically with paclitaxel [15, 17, 18, 27, 28]. In the current study, we evaluated the effects of IPAT on cell proliferation, apoptosis, and invasion along with paclitaxel synergy in USC cell lines. We further evaluated IPAT's ability to inhibit cell viability and induce apoptosis alone and in combination with paclitaxel in primary cell cultures of patient-derived USC. Our findings demonstrate that IPAT effectively targets phosphorylation of AKT to disrupt AKT/mTOR/S6 pathway, inhibits cell proliferation, induces apoptosis, and reduces invasion. Additionally, IPAT exhibits synergy with paclitaxel to inhibit cell proliferation in USC cell lines and primary cell cultures.

Activated *PI3K/AKT* and its downstream target mTOR are key signaling molecules involved in the control of cell proliferation, cell cycle arrest, apoptosis, and invasion in a variety of solid tumors. IPAT is highly selective for AKT binding and because it competes with ATP for binding sites, it prevents dephosphorylation of the p-AKT complex in a dose-dependent manner [15]. Increase in phosphorylation of AKT inhibits downstream signaling to biomarkers such as S6 and reduces cell proliferation in many preclinical models in vitro and in vivo [15, 17]. Consistent with prior works, we showed that IPAT increased AKT phosphorylation at Ser473 which subsequently decreased S6 phosphorylation in USC cells (**Figure 1B**, **1C**). Additionally, several studies in preclinical models implicate a crucial role of IPAT in induction of apoptosis and cell cycle arrest [15, 16, 29, 30]. In our USC cell lines, IPAT showed dose-dependent induction of apoptosis through intrinsic apoptotic and extrinsic apoptotic pathways. Previous studies reported that the anti-proliferative activity of IPAT is dependent on the activity state of AKT, and high AKT activity predicts sensitivity to IPAT in many cancer cell lines and mouse models [15, 28]. We show that expression levels of phosphorylated AKT and S6 were not associated with sensitivity to IPAT in primary cultures or USC cell lines. Our results may be related to the small number of samples tested or the unique molecular prolife of USC, both of which require further study and clarification.

Dysregulation of signaling transduction has been recently recognized as a major pathway regulating EMT and angiogenesis, and ultimately resulting in a more motile phenotype in endometrial cancer [31, 32]. Targeting of AKT by MK2206, an allosteric inhibitor of AKT, significantly inhibited tumor growth in a USC patient-derived xenograft model and reduced cell invasion in endometrial cancer cell lines [33]. Additionally, combination IPAT and dasatinib or sunitinib, activated CDC42-associated kinase 1 (ACK1) inhibitors, generated synergetic inhibition of cell proliferation and invasion in *KRAS*-mutant non-small-cell lung cancer (NSCLC) cells [30]. Using adhesion, transwell, and wound healing assays, we found for the first time that IPAT effectively suppressed cell adhesion, migration, and invasion of USC cells in a dose-dependent manner. The anti-invasive activity of IPAT was conceivably associated with the process of EMT, which was supported by down-regulation of N-Cadherin, Slug, and Snail protein expression on Western blotting. Our results show IPAT exhibits dramatic inhibition of USC cell invasion by targeting PI3K/AKT/mTOR signaling pathways and therefore may have anti-metastatic therapeutic potential in USC.

Genetic mutations driving activation of the PI3K/AKT/mTOR pathway contribute to the central mechanism involving chemoresistance in a variety of solid tumors including endometrial cancer [34, 35]. Combination treatments usually block crucial oncogenic pathways that involve drug resistance and therefore sensitize cancer cells to the cytotoxic agents [36]. Inhibition of AKT/mTOR signaling sensitizes cancer cells to paclitaxel in paclitaxel-resistant and sensitive cancer cell lines [37-39]. The PI3K inhibitor, NVP BKM-120, in combination with paclitaxel and carboplatin, synergistically suppressed tumor growth in an endometrial cancer xenograft model, independent of *PIK3CA* gene mutation [40]. Similar synergistic effects of IPAT and paclitaxel have been reported in breast cancer cells which were sensitized through induction of apoptosis [18]. We found that inhibition of the AKT/mTOR pathway by IPAT in combination with paclitaxel significantly enhanced cytotoxicity in USC cell lines and primary cultures, indicating that IPAT may improve on the efficacy of paclitaxel. As further evidence of this, recent phase I and II clinical trials have confirmed that IPAT in combination with paclitaxel is well tolerated and holds the promise of a progression free survival benefit in advanced breast cancer and other solid tumors harboring mutations in *PIK3CA/AKT* and *PTEN* [20, 21, 41, 42].

While the world of targeted therapies is expanding rapidly, agents available for endometrial cancer, and particularly USC, are lacking. Our results demonstrate that IPAT appears promising in USC. IPAT exhibits significant antitumor activity in USC cell lines and primary cultures, including inhibiting invasion and increasing synergy with paclitaxel. Multiple clinical trials are currently underway investigating IPAT in combination with traditional platinum-based regimens, anti-microtubule agents, and immunotherapies, particularly PD-1/PD-L1 inhibitors. One such trial, called EndoMAP, pairs multiple targeted agents, including IPAT, with the anti-PDL-1 monoclonal antibody atezolizumab for women with recurrent or persistent endometrial cancer (NCT04486352). While much data is forthcoming, completed studies support further investigation of IPAT alone and in combination with other targeted agents, particularly in the setting of difficult-to-treat recurrent and metastatic solid tumors such as USC.

Acknowledgements

This work is supported by: Endometrial Cancer Molecularly Targeted Therapy Consortium, Genentech supplied IPAT for these pre-clinical studies.

Disclosure of conflict of interest

None.

Address correspondence to: Dr. Victoria Bae-Jump, Division of Gynecologic Oncology, University of North Carolina at Chapel Hill, Chapel Hill, NC 27599, USA. Tel: 919-843-4899; Fax: 919-966-2646; E-mail: victoria_baejump@med.unc.edu; Dr. Chunxiao Zhou, Division of Gynecologic Oncology, Lineberger Cancer Center, University of North Carolina at Chapel Hill, Chapel Hill, NC 27599, USA. Tel: 919-966-3270; Fax: 919-966-2646; E-mail: czhou@med.unc.edu

References

[1] Siegel RL, Miller KD, Fuchs HE and Jemal A. Cancer statistics, 2022. CA Cancer J Clin 2022; 72: 7-33.

[2] Zhang L, Kwan SY, Wong KK, Solaman PT, Lu KH and Mok SC. Pathogenesis and clinical management of uterine serous carcinoma. Cancers (Basel) 2020; 12: 686.
[3] Salvesen HB, Carter SL, Mannelqvist M, Dutt A, Getz G, Stefansson IM, Raeder MB, Sos ML, Engelsen IB, Trovik J, Wik E, Greulich H, Bø TH, Jonassen I, Thomas RK, Zander T, Garraway LA, Oyan AM, Sellers WR, Kalland KH, Meyerson M, Akslen LA and Beroukhim R. Integrated genomic profiling of endometrial carcinoma associates aggressive tumors with indicators of PI3 kinase activation. Proc Natl Acad Sci U S A 2009; 106: 4834-4839.
[4] Mahdi H, Xiu J, Reddy SK and DeBernardo R. Alteration in PI3K/mTOR, MAPK pathways and Her2 expression/amplification is more frequent in uterine serous carcinoma than ovarian serous carcinoma. J Surg Oncol 2015; 112: 188-194.
[5] Catasus L, D'Angelo E, Pons C, Espinosa I and Prat J. Expression profiling of 22 genes involved in the PI3K-AKT pathway identifies two subgroups of high-grade endometrial carcinomas with different molecular alterations. Mod Pathol 2010; 23: 694-702.
[6] Hayes MP and Ellenson LH. Molecular alterations in uterine serous carcinoma. Gynecol Oncol 2010; 116: 286-289.
[7] Janku F, Tsimberidou AM, Garrido-Laguna I, Wang X, Luthra R, Hong DS, Naing A, Falchook GS, Moroney JW, Piha-Paul SA, Wheler JJ, Moulder SL, Fu S and Kurzrock R. PIK3CA mutations in patients with advanced cancers treated with PI3K/AKT/mTOR axis inhibitors. Mol Cancer Ther 2011; 10: 558-565.
[8] Cocco E, Lopez S, Black J, Bellone S, Bonazzoli E, Predolini F, Ferrari F, Schwab CL, Menderes G, Zammataro L, Buza N, Hui P, Wong S, Zhao S, Bai Y, Rimm DL, Ratner E, Litkouhi B, Silasi DA, Azodi M, Schwartz PE and Santin AD. Dual CCNE1/PIK3CA targeting is synergistic in CCNE1-amplified/PIK3CA-mutated uterine serous carcinomas in vitro and in vivo. Br J Cancer 2016; 115: 303-311.
[9] Bogani G, Ray-Coquard I, Concin N, Ngoi NYL, Morice P, Enomoto T, Takehara K, Denys H, Nout RA, Lorusso D, Vaughan MM, Bini M, Takano M, Provencher D, Indini A, Sagae S, Wimberger P, Póka R, Segev Y, Kim SI, Candido Dos Reis FJ, Lopez S, Mariani A, Leitao MM Jr, Raspagliesi F, Panici PB, Di Donato V, Muzii L, Colombo N, Scambia G, Pignata S and Monk BJ. Uterine serous carcinoma. Gynecol Oncol 2021; 162: 226-234.
[10] Bonazzoli E, Cocco E, Lopez S, Bellone S, Zammataro L, Bianchi A, Manzano A, Yadav G, Manara P, Perrone E, Haines K, Espinal M, Dugan K, Menderes G, Altwerger G, Han C, Zeybek B, Litkouhi B, Ratner E, Silasi DA, Huang GS, Azodi M, Schwartz PE and Santin AD. PI3K oncogenic mutations mediate resistance to afatinib in HER2/neu overexpressing gynecological cancers. Gynecol Oncol 2019; 153: 158-164.
[11] Lopez S, Schwab CL, Cocco E, Bellone S, Bonazzoli E, English DP, Schwartz PE, Rutherford T, Angioli R and Santin AD. Taselisib, a selective inhibitor of PIK3CA, is highly effective on PIK3CA-mutated and HER2/neu amplified uterine serous carcinoma in vitro and in vivo. Gynecol Oncol 2014; 135: 312-317.
[12] Blake JF, Xu R, Bencsik JR, Xiao D, Kallan NC, Schlachter S, Mitchell IS, Spencer KL, Banka AL, Wallace EM, Gloor SL, Martinson M, Woessner RD, Vigers GP, Brandhuber BJ, Liang J, Safina BS, Li J, Zhang B, Chabot C, Do S, Lee L, Oeh J, Sampath D, Lee BB, Lin K, Liederer BM and Skelton NJ. Discovery and preclinical pharmacology of a selective ATP-competitive Akt inhibitor (GDC-0068) for the treatment of human tumors. J Med Chem 2012; 55: 8110-8127.
[13] Roncolato F, Lindemann K, Willson ML, Martyn J and Mileshkin L. PI3K/AKT/mTOR inhibitors for advanced or recurrent endometrial cancer. Cochrane Database Syst Rev 2019; 10: CD012160.
[14] Saura C, Roda D, Roselló S, Oliveira M, Macarulla T, Pérez-Fidalgo JA, Morales-Barrera R, Sanchis-García JM, Musib L, Budha N, Zhu J, Nannini M, Chan WY, Sanabria Bohórquez SM, Meng RD, Lin K, Yan Y, Patel P, Baselga J, Tabernero J and Cervantes A. A first-in-human phase I study of the ATP-competitive AKT inhibitor ipatasertib demonstrates robust and safe targeting of AKT in patients with solid tumors. Cancer Discov 2017; 7: 102-113.
[15] Lin J, Sampath D, Nannini MA, Lee BB, Degtyarev M, Oeh J, Savage H, Guan Z, Hong R, Kassees R, Lee LB, Risom T, Gross S, Liederer BM, Koeppen H, Skelton NJ, Wallin JJ, Belvin M, Punnoose E, Friedman LS and Lin K. Targeting activated Akt with GDC-0068, a novel selective Akt inhibitor that is efficacious in multiple tumor models. Clin Cancer Res 2013; 19: 1760-1772.
[16] Sun L, Huang Y, Liu YY, Zhao YJ, He XX, Zhang LL, Wang F and Zhang YJ. Ipatasertib, a novel Akt inhibitor, induces transcription factor FoxO3a and NF-κB directly regulates PUMA-dependent apoptosis. Cell Death Dis 2018; 9: 911.
[17] LoRusso PM. Inhibition of the PI3K/AKT/mTOR pathway in solid tumors. J Clin Oncol 2016; 34: 3803-3815.
[18] Morgillo F, Della Corte CM, Diana A, Mauro CD, Ciaramella V, Barra G, Belli V, Franzese E,

Bianco R, Maiello E, de Vita F, Ciardiello F and Orditura M. Phosphatidylinositol 3-kinase (PI3Kα)/AKT axis blockade with taselisib or ipatasertib enhances the efficacy of anti-microtubule drugs in human breast cancer cells. Oncotarget 2017; 8: 76479-76491.

[19] Doi T, Fujiwara Y, Matsubara N, Tomomatsu J, Iwasa S, Tanaka A, Endo-Tsukude C, Nakagawa S and Takahashi S. Phase I study of ipatasertib as a single agent and in combination with abiraterone plus prednisolone in Japanese patients with advanced solid tumors. Cancer Chemother Pharmacol 2019; 84: 393-404.

[20] Isakoff SJ, Tabernero J, Molife LR, Soria JC, Cervantes A, Vogelzang NJ, Patel MR, Hussain M, Baron A, Argilés G, Conkling PR, Sampath D, Maslyar D, Patel P, Chan W, Gendreau S, Musib L, Xu N, Ma H, Lin K and Bendell J. Antitumor activity of ipatasertib combined with chemotherapy: results from a phase Ib study in solid tumors. Ann Oncol 2020; 31: 626-633.

[21] Dent R, Oliveira M, Isakoff SJ, Im SA, Espié M, Blau S, Tan AR, Saura C, Wongchenko MJ, Xu N, Bradley D, Reilly SJ, Mani A and Kim SB; LOTUS investigators. Final results of the double-blind placebo-controlled randomized phase 2 LOTUS trial of first-line ipatasertib plus paclitaxel for inoperable locally advanced/metastatic triple-negative breast cancer. Breast Cancer Res Treat 2021; 189: 377-386.

[22] Van Nyen T, Moiola CP, Colas E, Annibali D and Amant F. Modeling endometrial cancer: past, present, and future. Int J Mol Sci 2018; 19: 2348.

[23] Foucquier J and Guedj M. Analysis of drug combinations: current methodological landscape. Pharmacol Res Perspect 2015; 3: e00149.

[24] Braselmann H, Michna A, Heß J and Unger K. CFAssay: statistical analysis of the colony formation assay. Radiat Oncol 2015; 10: 223.

[25] Chan JJ, Tan TJY and Dent RA. Novel therapeutic avenues in triple-negative breast cancer: PI3K/AKT inhibition, androgen receptor blockade, and beyond. Ther Adv Med Oncol 2019; 11: 1758835919880429.

[26] Makker V, Green AK, Wenham RM, Mutch D, Davidson B and Miller DS. New therapies for advanced, recurrent, and metastatic endometrial cancers. Gynecol Oncol Res Pract 2017; 4: 19.

[27] Uko NE, Güner OF, Matesic DF and Bowen JP. Akt pathway inhibitors. Curr Top Med Chem 2020; 20: 883-900.

[28] Ippen FM, Grosch JK, Subramanian M, Kuter BM, Liederer BM, Plise EG, Mora JL, Nayyar N, Schmidt SP, Giobbie-Hurder A, Martinez-Lage M, Carter SL, Cahill DP, Wakimoto H and Brastianos PK. Targeting the PI3K/Akt/mTOR pathway with the pan-Akt inhibitor GDC-0068 in PIK3CA-mutant breast cancer brain metastases. Neuro Oncol 2019; 21: 1401-1411.

[29] Yu L, Liu ZS, Qiu L, Hao LL and Guo J. Ipatasertib sensitizes colon cancer cells to TRAIL-induced apoptosis through ROS-mediated caspase activation. Biochem Biophys Res Commun 2019; 519: 812-818.

[30] Yu XJ, Liu J, Qiu HW, Hao HT, Zhu JH and Peng SY. Combined inhibition of ACK1 and AKT shows potential toward targeted therapy against KRAS-mutant non-small-cell lung cancer. Bosn J Basic Med Sci 2021; 21: 198-207.

[31] Liu Z, Hong ZP and Qu PP. Proteomic analysis of human endometrial tissues reveals the roles of PI3K/AKT/mTOR pathway and tumor angiogenesis molecules in the pathogenesis of endometrial cancer. Biomed Res Int 2020; 2020: 5273969.

[32] Kent CN and Guttilla Reed IK. Regulation of epithelial-mesenchymal transition in endometrial cancer: connecting PI3K, estrogen signaling, and microRNAs. Clin Transl Oncol 2016; 18: 1056-1061.

[33] Winder A, Unno K, Yu Y, Lurain J and Kim JJ. The allosteric AKT inhibitor, MK2206, decreases tumor growth and invasion in patient derived xenografts of endometrial cancer. Cancer Biol Ther 2017; 18: 958-964.

[34] Guo FJ, Zhang HN, Jia ZH, Cui MH and Tian JY. Chemoresistance and targeting of growth factors/cytokines signalling pathways: towards the development of effective therapeutic strategy for endometrial cancer. Am J Cancer Res 2018; 8: 1317-1331.

[35] Brasseur K, Gévry N and Asselin E. Chemoresistance and targeted therapies in ovarian and endometrial cancers. Oncotarget 2017; 8: 4008-4042.

[36] McCubrey JA, Steelman LS, Chappell WH, Abrams SL, Franklin RA, Montalto G, Cervello M, Libra M, Candido S, Malaponte G, Mazzarino MC, Fagone P, Nicoletti F, Bäsecke J, Mijatovic S, Maksimovic-Ivanic D, Milella M, Tafuri A, Chiarini F, Evangelisti C, Cocco L and Martelli AM. Ras/Raf/MEK/ERK and PI3K/PTEN/Akt/mTOR cascade inhibitors: how mutations can result in therapy resistance and how to overcome resistance. Oncotarget 2012; 3: 1068-1111.

[37] Almhanna K, Cubitt CL, Zhang S, Kazim S, Husain K, Sullivan D, Sebti S and Malafa M. MK-2206, an Akt inhibitor, enhances carboplatinum/paclitaxel efficacy in gastric cancer cell lines. Cancer Biol Ther 2013; 14: 932-936.

[38] Li TY, Chen XN, Wan JQ, Hu XX, Chen WZ and Wang HX. Akt inhibition improves the efficacy of cabazitaxel nanomedicine in preclinical tax-

ane-resistant cancer models. Int J Pharm 2021; 607: 121017.
[39] Jabbarzadeh Kaboli P, Salimian F, Aghapour S, Xiang SX, Zhao QJ, Li MX, Wu X, Du FK, Zhao YS, Shen J, Cho CH and Xiao ZG. Akt-targeted therapy as a promising strategy to overcome drug resistance in breast cancer - a comprehensive review from chemotherapy to immunotherapy. Pharmacol Res 2020; 156: 104806.
[40] Bradford LS, Rauh-Hain A, Clark RM, Groeneweg JW, Zhang L, Borger D, Zukerberg LR, Growdon WB, Foster R and Rueda BR. Assessing the efficacy of targeting the phosphatidylinositol 3-kinase/AKT/mTOR signaling pathway in endometrial cancer. Gynecol Oncol 2014; 133: 346-352.
[41] Oliveira M, Saura C, Nuciforo P, Calvo I, Andersen J, Passos-Coelho JL, Gil Gil M, Bermejo B, Patt DA, Ciruelos E, de la Peña L, Xu N, Wongchenko M, Shi Z, Singel SM and Isakoff SJ. FAIRLANE, a double-blind placebo-controlled randomized phase II trial of neoadjuvant ipatasertib plus paclitaxel for early triple-negative breast cancer. Ann Oncol 2019; 30: 1289-1297.
[42] Kim SB, Dent R, Im SA, Espié M, Blau S, Tan AR, Isakoff SJ, Oliveira M, Saura C, Wongchenko MJ, Kapp AV, Chan WY, Singel SM, Maslyar DJ and Baselga J; LOTUS investigators. Ipatasertib plus paclitaxel versus placebo plus paclitaxel as first-line therapy for metastatic triple-negative breast cancer (LOTUS): a multicentre, randomised, double-blind, placebo-controlled, phase 2 trial. Lancet Oncol 2017; 18: 1360-1372.